Colloids and Surfaces A: Physicochem. Eng. Aspects 358 (2010) 13–20

Contents lists available at ScienceDirect

Colloids and Surfaces A: Physicochemical and Engineering Aspects

journal homepage: www.elsevier.com/locate/colsurfa

Characterization of monolithic porous carbon prepared from resorcinol/formaldehyde gels with cationic surfactant

M.M. Bruno[a], N.G. Cotella[a], M.C. Miras[a], T. Koch[b], S. Seidler[b], C. Barbero[a,*]

[a] Departamento de Química, Universidad Nacional de Río Cuarto, Agencia postal No. 3, 5800 Río Cuarto, Argentina
[b] Institute of Materials Science and Technology, Vienna University of Technology, Favoritenstrasse 9-11, A-1040 Vienna, Austria

ARTICLE INFO

Article history:
Received 31 October 2009
Received in revised form
22 December 2009
Accepted 7 January 2010
Available online 15 January 2010

Keywords:
Porous carbon
Resins carbonization
Electrochemical properties
Mechanical properties

ABSTRACT

Monolithic polymer precursor of porous carbon was produced from polymerization of resorcinol–formaldehyde (RF) in the presence of cationic surfactant. The influence of concentration of the surfactant template, present in the sol–gel polymerization, on the electrochemical capacity was investigated by electrochemical impedance. It was found that a threshold concentration of surfactant is necessary to obtain sizable capacitance values. However, at higher concentrations of the surfactant, the capacitance values do not change significantly. The porous carbons have a large specific surface area (up to 671 m^2/g). They also show large specific (up to 150 F/g) and volumetric capacitances (up to 130 F/cm^3), in acid media. The carbon produced from the molar concentration of 0.32 M of surfactant (called carbon mesogel) was studied in detail. The products obtained from the polymerization and the thermal decomposition of the surfactant were further identified by TGA/MS analysis. The mechanical properties of the porous material show a good correlation with the values expected from the porosity present in the carbon matrix.

1. Introduction

Nanostructured carbon materials are used in many areas of modern science and technology due to their properties, such as high specific surface areas, large pore volumes, chemical inertness, and good mechanical stability. In the case of nanostructured glassy carbon, they also have good electronic conductivity. Carbon materials are especially suitable for use in electrical double-layer capacitors (EDLCs) and other energy storage devices [1]. Conventional capacitors store energy electrostatically on two electrodes separated by a dielectric, the capacitance of which is $C = \varepsilon A/d$, ε being the dielectric constant, A the surface area, and d the dielectric thickness. In a double-layer capacitor, charges accumulate at the boundary between electrode and electrolyte to form two charge layers with a separation of several Angstroms. Constructed with electrodes made of high surface area materials, EDLCs are therefore able to achieve energy densities considerably higher than those offered by electrostatic capacitors.

One of the most important features of carbon materials is the possibility to get high specific surface area. Therefore, porous materials with surface areas in the range of 400–2000 m^2/g, such as activated carbon (powder or fiber cloths) [2,3], carbon nanotubes [4] or carbon aerogels [5], are ideal materials for making EDLCs. Since, in several experimental results, was found that only a fraction of the ideal capacitance can typically be achieved in the experiments [6,7] it was assumed that hydrated ions can penetrate micropores [8–9] or electrical double-layer overlapping inside the pose prevents energy storage in micropores [10]. However, it has been shown recently those micropores of diameter as small as ca. 0.7 nm can contribute significantly to electric double-layer capacitance [11]. To explain that behavior, it was assumed that the ions line up inside the micropores forming a 'electric wire in cylinder' model of a capacitor. As it is clearly discussed in Ref. [11], such mechanism override the limitation inherent in a purely double-layer model allowing smaller pores to contribute significantly to the specific capacitance. The capacitance it also affected by the pore surface chemistry [12,13]. The presence of hydrophilic groups, e.g. oxygen functionalities, on the carbon surface improves the wettability of the material by an aqueous electrolyte resulting in a better penetration of ions within the porous structure. Moreover, some redox active oxygen surface functionalities (e.g. quinones) induce a pseudocapacitance which leads to an enhancement of the capacitance [14,15].

High surface area carbon materials containing tailored pore distribution on porous materials and regularly interconnected pores are particularly desirable for the EDLC electrode [16,17]. One way to synthesize those materials is to produce porous precursor resins, such as resorcinol–formaldehyde (RF), which are then converted into porous glassy carbon by carbonization (heating in inert atmo-

* Corresponding author. Fax: +54 358 4676233.
E-mail address: mbruno@exa.unrc.edu.ar (C. Barbero).

0927-7757/$ – see front matter © 2010 Elsevier B.V. All rights reserved.
doi:10.1016/j.colsurfa.2010.01.017

sphere). From the methods and processing conditions used in the synthesis, it is possible to affect the final structure of the gel. Ambient air drying of RF gels gives xerogels, without open pores, by the collapse of the gel due to surface tension forces at the water/air interface. To avoid the collapse, the gels could be dried using supercritical liquids (aerogels) [18] or low surface tension solvents (ambigel) [19]. In both cases, the small surface tension forces do not collapse the gel pores. Another way involves sublimation of the solvent from the pores by lyofilization of the gels (cryogels) [20]. Alternatively, mesoporous inorganic matrices could be used to template the pores in the resin [21].

In recent years, there has been a recognition that self-assembled molecular systems can serve as templates in the synthesis of nanostructured materials [22]. Since 1992, a new family of ordered mesoporous inorganic materials has attracted considerable and still growing attention due to their fascinating structures and wide application perspectives [23,24]. These materials with a tailored size pore distribution may be engineered using a variety of micelles of surfactant molecules as templates. They are produced in various compositions, such as oxides (e.g. silica, alumina, titania, zirconia, mixed oxides) by condensation of inorganic species around the arrays of self-assembled aggregates of surfactant molecules in water [25,26].

From the synthesis of RF organic sol–gel according to a hydrolysis condensation reaction mechanism, that is analogous to the synthesis of inorganic oxides, Bell and Dietz reported the preparation of porous RF resins using surfactant micelles as templates which are eliminated during carbonization [27]. The material could be air dried without significant contraction. This method is less expensive than the formation of carbon aerogel with the use of supercritical fluids. The method is effective; however, the mechanism of pore formation using micelles of surfactants in RF gel is not clear whether it be similar to the proposed for oxides synthesis.

In the present work, a detailed study of the effect of surfactant concentration on the porous carbon electrochemical capacity is performed. Finally, the electrochemical response, scanning electron microscopy (SEM), thermogravimetric analysis coupled with mass spectroscopy (TGA/MS) and nanoindentation were used to characterize the monolithic porous carbon obtained with 0.32 M surfactant concentration.

2. Experimental

2.1. Preparation of mesoporous carbons

A precursor solution was prepared from surfactant (S), resorcinol (R), formaldehyde (F), Na_2CO_3 (C) and deionized water (W). Cationic surfactant, cetyltrimethylammonium bromide (CTAB, BDH), was used in this study. The solution was prepared mixing CTAB, resorcinol (Fluka), formaldehyde (37 wt %, Cicarelli), and Na_2CO_3 (Cicarelli) from 0.4 M aqueous solution. The molar ratio on the solution was fixed to F/R: 2, C/R: 5×10^{-3} and W/R: 10. The S/R molar ratio was varied in the work. The mixture was stirred and heated over the Kraft temperature of the surfactant. At this moment, the solution became translucent. Then it was heated at 70 °C for 24 h at atmospheric pressure. The brown monolithic RF polymer was dried at 70 °C in air for 6 h. Finally, it was carbonized under a N_2 atmosphere at 800 °C with a heating rate of 40 K h^{-1}.

2.2. Characterization measurements

The electrochemical performance of the mesogel carbon electrodes was analyzed with a three-electrode configuration. The monolithic samples were machined with a thickness of 0.3 mm and ca. 10 mg of weight. A carbon aerogel (Maketech, geometrical area 5 times of the working electrode) and a silver/silver chloride electrode (saturated KCl) were used as counter and reference electrode. Cyclic voltammetry (CV) and the AC impedance measurements were performed using a PC4 Potentiostat-Galvanostat-ZRA (Gamry Instruments, Inc.). The electrolyte was aqueous 1.0 M H_2SO_4 and 0.5 M NaF unless otherwise specified. The current in the resulting cyclic voltammograms was divided by the scan rate and the electrode mass to obtain specific capacitance vs. voltage profiles. AC impedance measurements were made over the range from 5×10^4 to 3×10^{-3} Hz with a sinusoidal perturbation of 1 mV of amplitude, 4 points per decade change in frequency.

A resting time of at least 15 min at each potential was used before measuring the EIS spectra. A pre-treatment called "burn in" was performed on the carbon electrodes. It consists of anodic oxidation (15 min at 1.35 V) followed by cathodic reduction (15 min at 0.2 V). Subsequently, at least 10 CVs cycles were carried out to stabilize the surface. This slow oxidation on the carbon enhances the carbon response.

The surface area and pore size distribution were calculated from nitrogen adsorption isotherms (Micrometrics, ASAP 2000) using the Brunauer, Emmett, and Teller (BET), and Barrett, Joyner and Halenda (BJH) methods, respectively. The morphology of the carbons was observed with a scanning electron microscope (SEM, Philips 515). Thermogravimetric (TG) studies were carried out with a TGA 2050 (TA-Instruments, USA). Typically samples of about 10 mg were heated under air and nitrogen atmosphere of 165 mL/min gas stream at a heating rate of 10 K/min. The TGA/MS studies were carried out by coupling the TGA 2050 (TA-Instruments, USA) and a quadrupole mass spectrometer (Thermostar, Balzers, LI) with electron ionization and Channeltron detector. The coupling consisted of a quartz capillary tube enveloped by a heated jacket.

The density of the porous carbon, measured from the ratio of weight to geometric volume, is 0.89 (±0.01) g/cm^3.

The nanoindentation tests were carried out with Nanoindenter XP (MTS Systems, USA, with Berkovich Indenter) equipment at a rate of 50 nm/s up to an indentation depth of 1 μm. At maximum load a holding segment of 30 s was applied followed by the unloading. The indentation hardness H_{IT} and modulus E_{IT} were calculated according to ISO 14577. The projected contact area is calculated by the method of Oliver and Pharr [28].

3. Results and discussion

3.1. Correlation between double-layer capacitance and surface area

The presence of this large amount of oxygenated groups in the surface of the activated carbon can affect the capacitance of the material mainly in two different ways: the oxygenated groups can improve the wettability of the carbon surface, which is very important to maximize the access of the electrolyte to the surface of carbon, and the presence of redox oxygenated groups (e.g. quinones) means that pseudocapacitance arises from faradaic charge transfer reactions on the surface [13]. It is likely that the amount of oxygenated groups is affected by the carbonization parameters. For these reasons, to analyze the effect of the surfactant concentration on surface area using capacitance measurements the carbonization conditions were maintained constant in this work. Thus, the amount of surface functionalities were considered to be proportional to the surface of the carbons generated.

The ratio of surfactant/resorcinol (S/R) used in the synthesis range from 0 to 0.12. Where S/R = 0.12 represents 0.61 M of CTAB in the polymerization media. At higher concentration of surfactants, two phases were observed in the polymerization reaction.

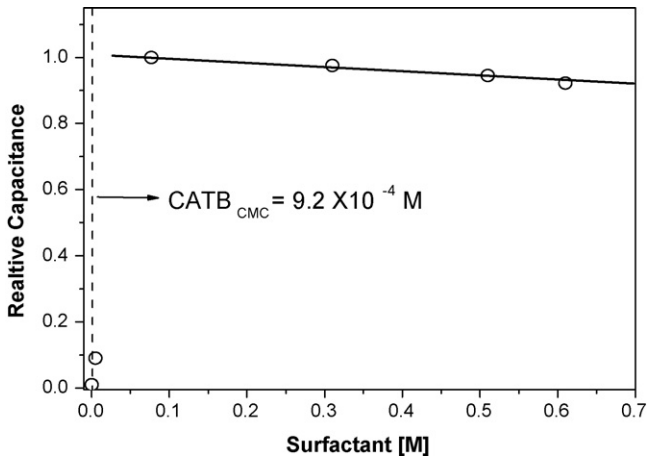

Fig. 1. Specific capacitance values of different mesoporous carbons measured with a frequency of 3 mHz, at 0.35 V, in 1 M H_2SO_4.

The RF gel did not shrink noticeably upon drying. In the resin state, it was easy to machine. All the carbons obtained using these methods were monolithic.

The specific capacitance of the different carbons obtained could be calculated from the Electrochemical Impedance Spectroscopy (EIS) measurements. At high frequency, only the outermost area is accessed by the measurement. But at low frequency, all the surface area is accessed by the measurement (Fig. 4b) [29]. The capacitance was calculated from the impedance values measured at low frequency (3 mHz), using Eq. (1):

$$C = \frac{1}{2\pi f Z''} \quad (1)$$

where i, f and Z'' (f) are the imaginary unit, AC frequency and complex impedance at a frequency, respectively.

As we will see (below) the capacitance varies with the electrode potential. Therefore, the measurements were all made at 0.35 V, in 1 M H_2SO_4.

In Fig. 1 the relationship between specific capacitance and the surfactant concentration are shown. The values were normalized to the maximum value of capacitance for the carbons obtained of 150 F/g. The capacitance values calculated for the carbons produced below 0.077 M are practically negligible. Above this molar ratio the capacitance increases notably and it does not show a marked change (less than 5%). These results show that a threshold concentration is necessary to obtain a sizable surface area of the carbon and that is close to critical micellar concentration (CMC) of CTAB in pure water [30]. Many models have been proposed to explain such behavior [31–33]. The existence of a critical micelar concentration or the existence of a minimal concentration of the cationic surfactant would indicate that micelle of surfactant is necessary to form nanostructurated materials but these results are not clear yet. Fig. 2a shows the N_2 adsorption isotherms of carbons obtained with a molar concentration of 0.077 M and 0.61 M. Those concentrations correspond to the samples in the extreme points of the range of specific maximum capacitance (Fig. 1).

The BET surface area of the samples was calculated to be 671 m^2/g (0.077 M) and 576 m^2/g (0.61 M). In both cases, the pore size distribution shows a monomodal distribution where the maximum shifted to larger pores when the surfactant concentration increased (Fig. 2b). The monomodal shape might indicate that a template effect by the surfactant is operative. While the surface area decreases ca. 100 m^2/g, when the surfactant concentration increases, the amount of ultramicropores (pores of diameter below 0.7 nm) remains the same. On the other hand, the area due to wider micropores (d >0.7 nm) decreases somewhat when the surfactant

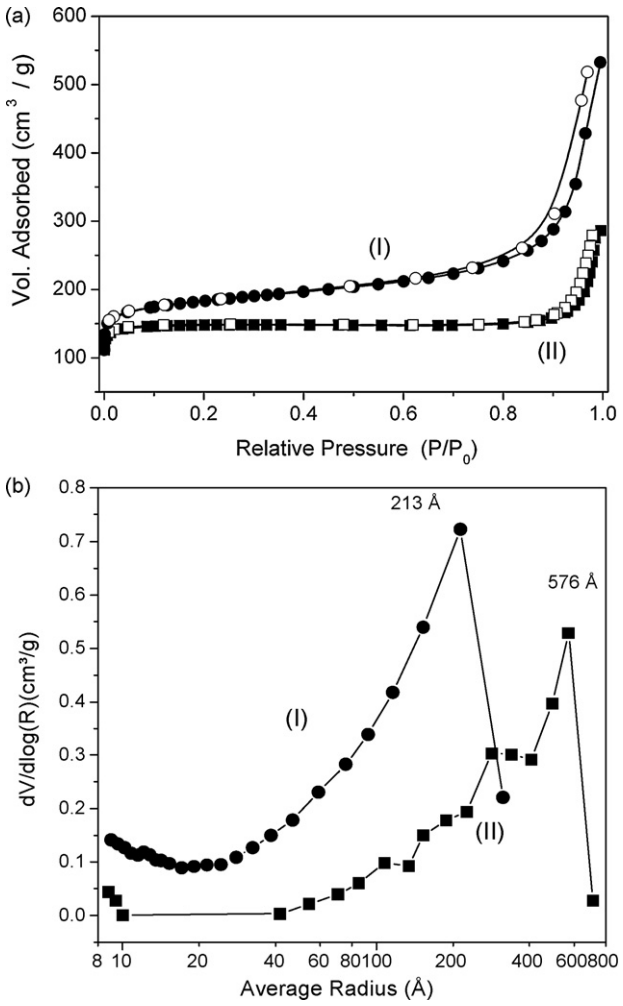

Fig. 2. (a) Nitrogen adsorption and desorption isotherms of carbons produced [CTAB] = 0.077 M (I) and 0.61 M (II). (b) Pore volume distribution (BJH) curves obtained from a.

concentration increases. This behavior probably accounts for the slight decrease in specific capacitance values observed for the different carbons. While such behavior does not allow tailoring the capacitance by changing the surfactant concentration, it makes the synthetic procedure very robust with respect to variations in effective surfactant concentration.

To analyze the general properties of the porous glass carbon, the material obtained with a [CTAB] = 0.32 M (called subsequently carbon mesogel) was chosen.

3.2. Characterization of carbon mesogel

3.2.1. Electrochemical characterization

Fig. 3 shows the cyclic voltammetric response for a carbon mesogel in 1 M H_2SO_4 (scan rate: 1 mV/s). The Y-axis of the curve was expressed as specific capacitance (C_{sp}) using the Eq. (2):

$$C_{sp} = \frac{i}{v \times m} \quad (2)$$

where i is the current, v is the scan rate and m is the electrode mass.

The voltammogram reveals a large specific capacitance in a broad wave with maxima at ca. 0.35 $V_{Ag/AgCl}$. The wave observed is likely to be due to the oxidation/reduction of quinone-like functionalities (Eq. (3)) present on the carbon surface.

$$QH_2 \rightleftharpoons Q + 2H^+ + 2e^- \quad (3)$$

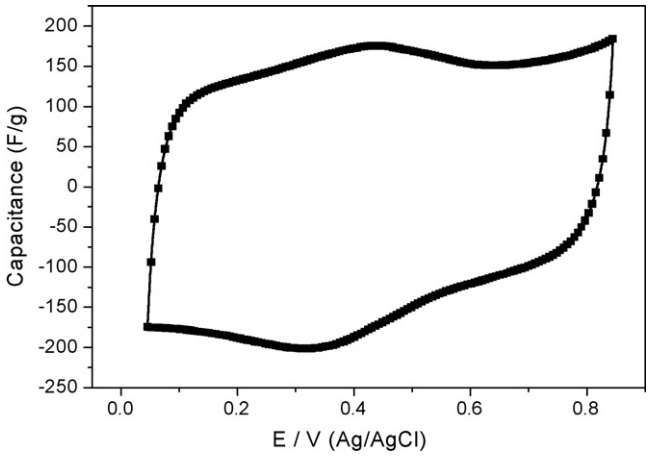

Fig. 3. Cyclic voltammogram of a carbon mesogel electrode in 1 M H_2SO_4. Scan rate: 1 mV s^{-1}.

An alternative way to obtain the specific capacitance is using the Eq. (4), where the current is integrated and divided by the whole potential window, i.e.:

$$C_{sp} = \frac{\int idt}{\Delta V \times m} \quad (4)$$

where i is the current, ΔV the potential window and m the mass of the electrode.

The specific capacitance calculated with this method for the voltammogram in Fig. 3 is of ca. 145 F/g. The corresponding volumetric capacitance is of ca. 125 F/cm^3.

Fig. 4a presents the impedance spectrum of carbon mesogel at 0.35 V in H_2SO_4 1 M. The Nyquist plots exhibit a capacitive behavior in the low-frequency range with a quite vertical dependence of the imaginary part vs. the real impedance part. The resistance changes weakly with the frequency and the capacitor behavior tends to approach that of a pure capacitance.

The frequency-dependent capacitance obtained following the Eq. (1), are plotted in Fig. 4b. According on the De Levie transmission line model of a porous electrode with straight pores considered as cylindrical capillaries. The frequency-dependent capacitance of porous electrodes can be analyzed [34,35]. The parameter 'penetration depth (l)' is calculated using Eq. (5):

$$l = \frac{1}{\sqrt{\pi f R' C'}} \quad (5)$$

where R' is the pore resistance and C' is the pore capacitance per unit pore length.

It is useful to understand the impedance behavior of porous electrodes. This equation reads that, when the ac frequency is sufficiently high for the penetration depth to be smaller than the pore length (lp) of the porous electrodes, only the outer surface (near pore opening) is influenced by the ac voltage signal [1]. As a result, a small capacitance is observed because only a limited part of electrode surface is utilized as a capacitor. In the low-frequency extreme, where the condition $l > lp$ holds, most of the pore surface is utilized as a capacitor and results in a maximum capacitance. Based on this discussion, the frequency-dependent capacitance shown in Fig. 4b can be explained. The transmission line model appears to be valid in the present electrode systems because the carbon used is mesoporous. It is first assumed that utilization of the pore surface, where the EDLC component of the carbon surface are developed, is 100% at the low-frequency limit (3 mHz) but zero at the high-frequency limit. This assumption is made based on the relation between the penetration depth (l) and the pore length (lp) of porous electrodes.

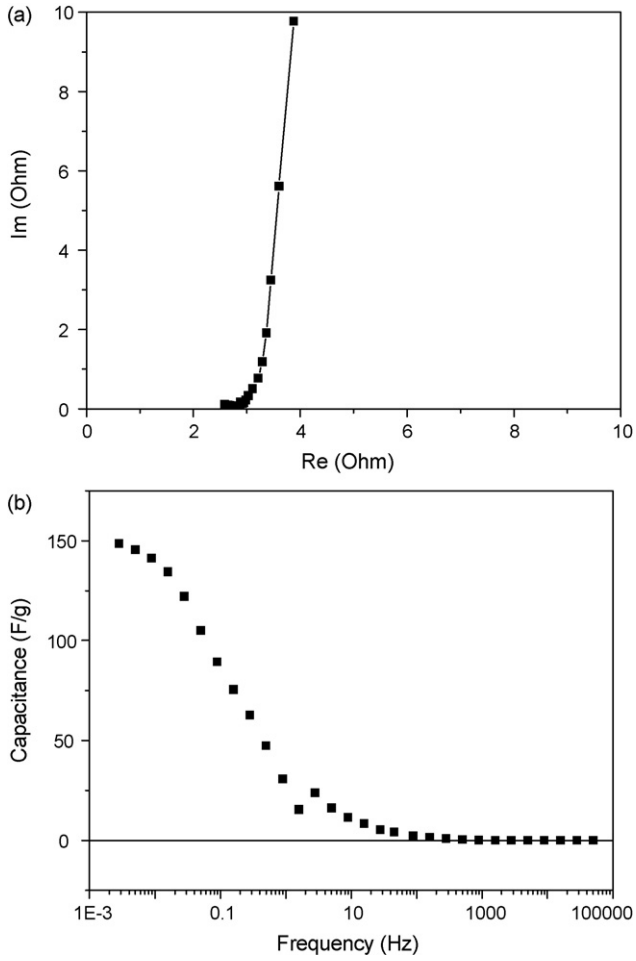

Fig. 4. (a) Typical Nyquist plot for mesogel electrode. Frequency range is 5×10^4 to 3×10^{-3} Hz. (b) Frequency-dependent capacitance profiles.

Fig. 5 shows the values of specific capacitance as a function of the measurement potential in 1 M H_2SO_4.

The specific capacitance depends on the electrode potential with a maximum value of ca. 145 F/g at 0.35 V Ag/AgCl. In this system a considerable part of the capacitance is attributed to charge storage in redox groups, giving rise to pseudocapacitive behavior.

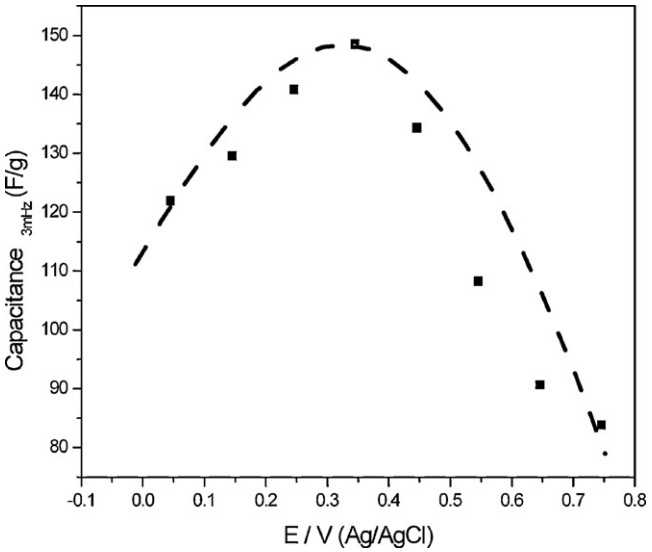

Fig. 5. Specific capacitance values measured at 3 mHz, in 1 M H_2SO_4.

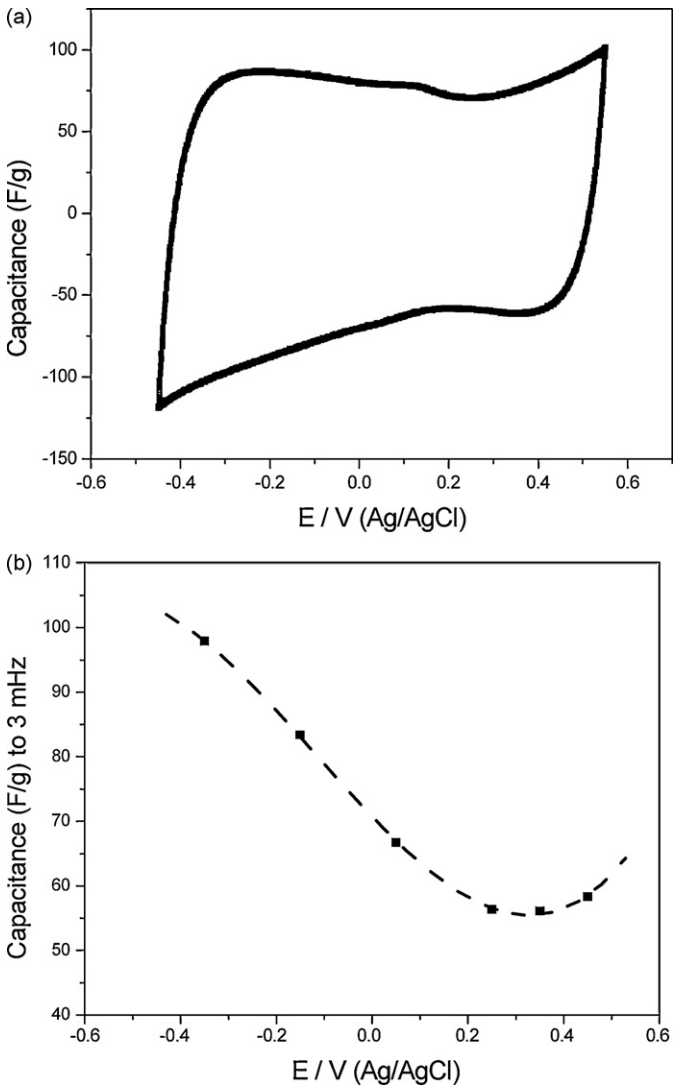

Fig. 6. (a) Cyclic voltammogram of a carbon mesogel electrode in NaF 0.5 M. Scan rate: 1 mV s^{-1}. (b) Specific capacitance in potential function measured at 3 mHz in 0.5 M NaF.

Similar behavior was reported for carbon–carbon composite produced by carbonization of resorcinol–formaldehyde (RF) resins formed on a commercial cellulose fiber [36]. The carbon mesogel was obtained using the same method of carbonization. This dependence of specific capacitance on potential is different from the one observed for carbon aerogels, where almost no dependence was observed in acid media [37].

0.5 M NaF was used in electrochemical characterization of porous carbon. This electrolyte has not specific adsorption and the quinones groups are inactive on the carbon in this potential range [38]. Thus, electrochemical double layer is build only from electrostatic factors. Fig. 6a shows a cyclic voltammogram with the typical "butterfly" appearance. Similar results were observed for carbon electrodes in Et_4NBF_4 in acetonitrile [6,39,40]. The values of specific capacitance as a function of the measurement potential measured to 3 mHz are plotted in the Fig. 6b. The plot has a parabolic shape, with a minimum value at 0.3 V Ag/AgCl which should correspond to the potential of minimum charge of the material. Interesting discussion were presented by some authors about this behavior, which can be attributed to electronic conductance of carbon and/or electrostatic interactions of ionic solutions side in the formation of double layer (Gouy Chapman theory) [6,39,40].

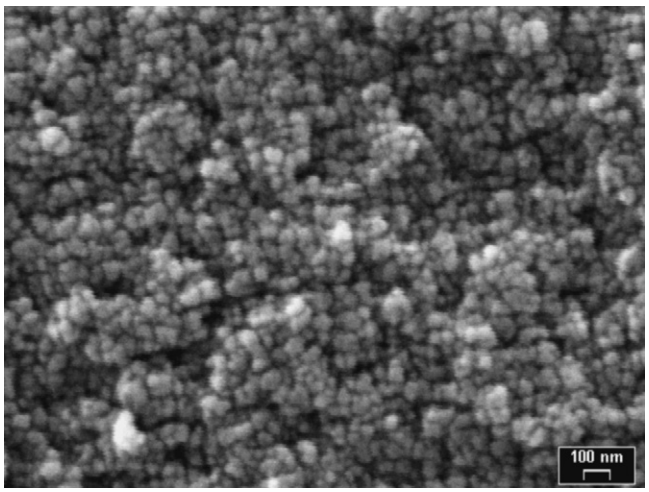

Fig. 7. SEM micrograph of the surface of carbon prepared with a 0.32 M surfactant concentration.

From cyclic voltammetry measurements, the specific capacitance was calculated following the Eq. (4). A value of the mean specific capacitance of 70 F/g is determined in that way. The corresponding value of volumetric capacity is of ca. 60 F/cm^3.

From subtraction between the capacitance values obtained in acid sulfuric and sodium fluoride media is possible to calculate the pseudacapacitance contribution. This value is around 50% of the total contribution in acid media. It suggests that pseudocapacitance related to the faradaic reaction in Eq. (1) has an important contribution to the specific capacitance of the material.

3.2.2. Scanning electronic microscopy (SEM)

Fig. 7 shows the SEM of a fractured mesogel carbon. There is no defined order, porous channel system or distinct superstructures on the carbon, as it would be expected with templates made of surfactant micelles. On the other hand, small globular forms (nanoparticles), separated by thin slits, are clearly appreciated.

The globular forms have sizes varying from 20 to 50 nm (average 45 nm). It seems that the slit holes left between the packing of the globular structures and the aggregations correspond to meso and macropores of the carbon, respectively. It was demonstrated that during the carbonization of phenolic resins, the destruction of the crosslink occurs between 450 and 750 °C, leading to the clustering of the aromatic units [41,42]. The globular structures observed could be assigned to those clusters.

In this large size of globular forms it would be possible to develop the space-charge region without overlapping within the nanoparticle of carbon [39]. For this reason, the variation of electronic conductance of the carbon could be discarded for this material.

3.2.3. TGA and TGA/MS measurements

As it was observed above, the carbonization plays an important role on the formation of the porous structure. Therefore, the carbonization process was studied using thermogravimetric analysis coupled with mass spectroscopy. Fig. 8a and b shows the normalized differential mass change (d(M)/dT) and the profile of mass to charge ratio (m/z) of the volatile products formed during the temperature scan, in nitrogen atmosphere, of a RF–surfactant resin (mesogel), RF resin without surfactant and pure surfactant (CTAB).

The DSC curve of CTAB presents an endothermic process around 270 °C due to its thermal degradation (not shown). The weight loss around 270 °C was observed for the CTAB compound and for the mesogel resin. This result suggests that this peak in the RF–surfactant curve can be attributed to CTAB decomposition. The

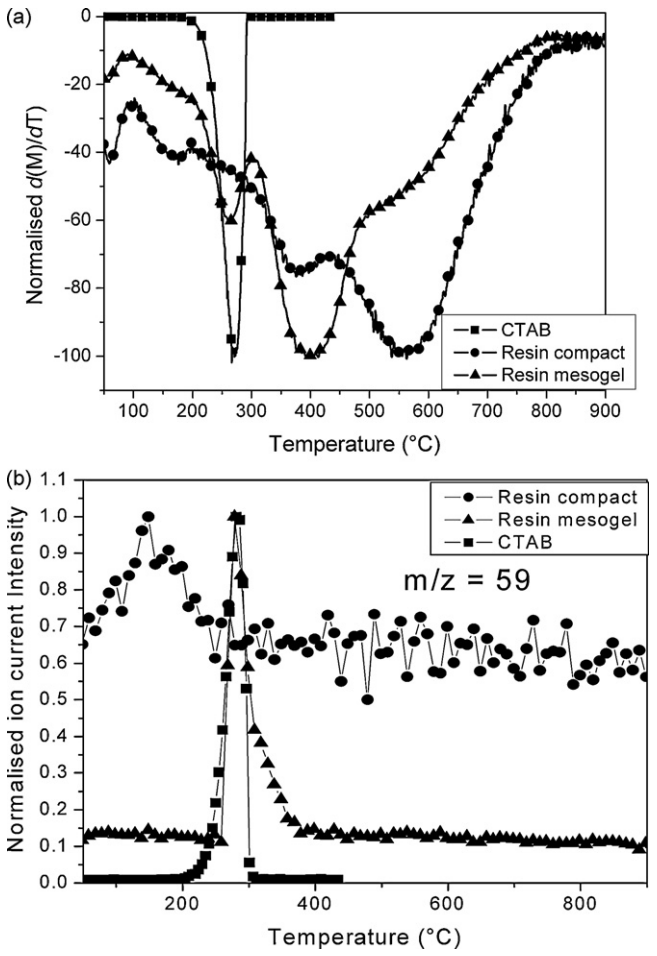

Fig. 8. (a) Normalized d(M)/dT profile. (b) Profile of trimethylammonium species (m/z = 59) during thermal decomposition of RF–surfactant resin, RF without surfactant resin and CTAB in N_2 atmosphere.

different profile of the d(M)/dT curve between a RF resin and a mesogel resin is probably due to the effect of the porous structure on the release of gaseous products.

Coupling the TGA with a mass spectrometer was possible to monitor the CTAB decomposition. The production of the trimethylammonium ion (m/z = 59) during thermal decomposition of the compact resin, mesogel resin and CTAB compound is shown in Fig. 6b. The profiles show that trimethylammonium ion detection begins at the same temperature in the mesogel resin and the CTAB. However, the profile of the mesogel shows a tail at higher temperatures indicating that relatively free and more trapped CTAB ions are present in the resin. Fragments of larger masses (90–105 m/z) were detected RF mesogel carbonization, probably be due to the destruction of crosslink and oligomers in the resin.

It is shown that CTAB ions are still retained in the RF matrix and decomposes during carbonization. The carbonizations processes of porous and compact RF resin are similar but the porous material carbonizes at lower temperatures.

3.2.4. Nanoindentation

The determination of mechanical properties of the material is essential for the design the analysis of performances and reliability of components. Nanoindentation-based techniques are an excellent method for measuring mechanical properties of small regions; especially modulus of elasticity, hardness and fracture toughness can be extracted from the indentation load vs. displacement curve for a variety of carbonous materials [43].

Table 1
Indentation modulus and hardness of the synthesized carbons materials.

Specimen	Indentation modulus E_{IT} [GPa]	Indentation hardness H_{IT} [GPa]
Carbon mesogel	6.6 ± 0.3	0.93 ± 0.07
Compact carbon	22.7 ± 0.5	3.74 ± 0.08
Porous matrix calculated by Rice's model	6.56 ± 0.14	1.08 ± 0.02

In the cases of porous material, the mechanical properties characterization is more complex than in compact materials, since the carbon mesogel has a morphology consisting of spherical particles (clusters) joined by discrete necks, as it can be observed in Fig. 7.

The mechanical properties are functions of the porosity of the material (size and pore distribution). In general, the resistance to indentation increases with decreasing initial porosity [44]. Furthermore, the hardness increases with penetration depth as a result of densification of the material [45]. Local densification of the porous material shows plastic deformation behavior and it would result in a significant error [46,47].

It has been shown that nanoindentation is a suitable technique for measuring mechanical properties of porous materials. Nevertheless it is necessary to take into account the effect of the densification produced during the measure, because it has a significant impact on the hardness value obtained [46].

For nanoindentation measurements, the samples were supported in polymer resin and its surface was polished. Fig. 9 shows the load vs. displacement curve of the nanoindentation measurements for carbon compact (like reference) and carbon mesogel.

Under loads below of 50 mN the carbons show elastic-plastic behavior in the indentation cycle. The force–displacement behavior for all these materials exhibits almost complete recovery with hysteresis between loading and unloading, which is a common feature of graphitic materials, the hysteresis upon unloading could be outcome of friction between the carbonous interlayer of vitreous carbon [48,49]. The residual penetration depth is caused by the irreversible plastic deformation [50]. In this case, the unloading path does not completely retrace the loading path but returns near the origin hysteretically.

Since carbon mesogel is a porous material, densification of the material upon compression should be taken into account to analyze the nanoidentation profile. However, in Fig. 9 can be observed that the residual plastic deformation, occurring immediately after the indentation, is comparable to that presented by compact glassy carbon which is around 300 nm. These results indicate that during the measurements the damage in the necks that bond the nanoparticles (densification effect) could be neglected.

Table 1 shows the indentation modulus and hardness calculated from the measurements. The calculation of hardness and elastic modulus was according to Oliver and Pharr model [51]. In this case, the contact area was calculated proposing an elastic model in which plastic pileup is neglected. ν = 0.3 was assumed for this carbons materials [52,53].

The compact carbon, used as reference material, shows hardness and elastic modulus values similar to those reported in the literature [43,54]. The hardness and elastic modulus of carbon mesogels values are lower than those of compact carbon. This is to be expected due to the lower amount of solid material in the former.

The mechanical properties of porous materials have been extensively studied to explain the property behavior of various materials, including those prepared by sol–gel processing [44,55–59]. Analyzing the structural conformation of the material, the hardness and modulus of porous carbon was estimated using the model of mini-

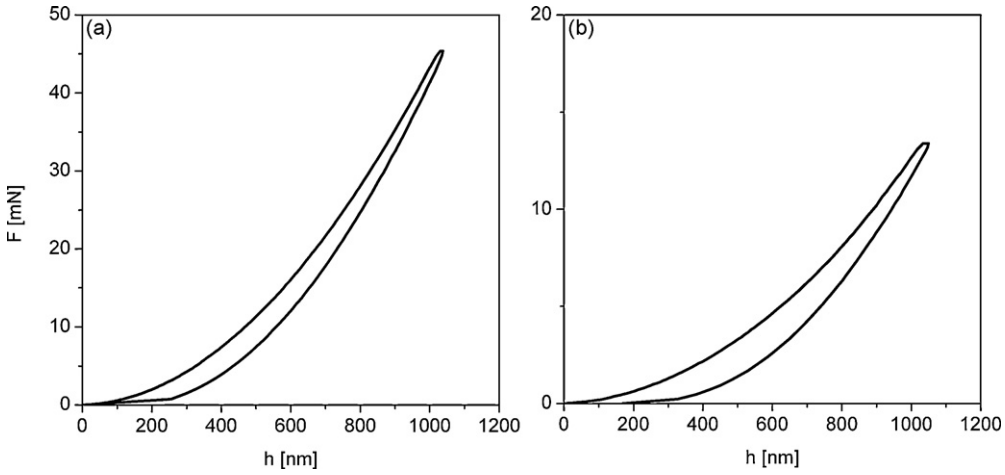

Fig. 9. Load–displacement curves obtained for monolithic materials, (a) compact carbon and (b) mesogel carbon.

mum solid area proposed for Rice [58,59]. It Assume that the porous material is formed for the packed of spherical particles. The model supposed the exponential dependence with the porosity as exp(*bf*), where *f* is the volume fraction of pores and *b* is a parameter characterizing the shape and distribution of pores. The value $b \sim 3.2$ was proposed for Rice to glassy carbon materials [59], and *f* was calculated from the density of both materials. The apparent density of compact carbon, produced in the same conditions but in absence of surfactant, and carbon mesogel were measured directly, as the ratio of weight to geometrical volume, to be 1.45 and 0.89 g/cm^3, respectively. The experimental mechanical properties values (Table 1) obtained are close to the values calculated from Rice's model. This result shows that the weakening of carbon mesogel is due only to the porosity of material. Such behavior of carbon mesogel is quite important because an additional weakness, which could be produced for destruction of crosslinks between the nanoparticles that compose the monolithic material, is not observed.

4. Conclusions

The carbonization of RF resins containing a cationic surfactant (CTAB) produces the formation of monolithic porous carbons. The pore distribution analysis of N_2 isotherm data shows that the material presents micro and mesopores. Changing the concentration of CTAB during the synthesis it is possible to form nanostructurated carbon with specific surface areas (S_{BET}) from 576 to 671 m^2/g. The increment of surfactant concentration shifts the pore size distribution to higher size diameters.

CTAB ions are still retained in the RF matrix after drying and decompose during carbonization. The carbonization processes of porous and compact RF resin are similar but the porous material carbonizes at lower temperatures.

The impedance measurement allows analyzing the correlation between the electrochemical active surface and the textural properties (BET surface area (S_{BET}) and pore distribution). Above a threshold surfactant concentration (ca. 1 mM) the capacitance developed is large. While the S_{BET} decreases, the pore size increases. The specific capacitance only decrease slightly when higher surfactant concentration is used. This may be explained by the fact that the area due to wider pores (d >0.7 nm), remains almost unchanged while the S_{BET} area changes.

The porous carbon presents, in aqueous sulfuric acid, a specific capacitance of around 145 F/g and a volumetric capacitance of ca. 129 F/cm^3. The value is comparable to other reported previously [11], while the volumetric capacitance is significantly (>50%) larger than those reported previously probably due to the compact nature of the monolithic carbon. This result makes the material especially suitable to be used in volume constrained devices like microelectronic systems. A comparison with the values measured in neutral aqueous solution (ca. 50% lower) suggests that pseudocapacitive contribution of the surface redox groups is operative in acid media. It is likely that oxygenated (quinone like) groups on the surface are involved in the pseudocapacitance.

The mechanical properties of carbon mesogel are in agreement with the Rice's model for porous solid materials, it show a closer value to the expected from the porosity present in the carbon matrix.

It is possible to conclude that the cationic surfactant, at concentration higher than ca. 1 mM, is effective to induce the presence of porosity in the carbon material. However, a templating effect by cylindrical micelles seems not to be operative. The actual mechanism of surfactant effect is not clear at this stage, and further studies are being carried out in our research group to clarify the issue.

Acknowledgements

Valuable discussions with D. Acevedo are gratefully acknowledged. This work was funded by FONCYT, CONICET, SECYT-UNRC and ADEMAT Network (ALFA-EU). M. Bruno thanks CONICET for a graduate research fellowship. C. Barbero is a permanent research fellow of CONICET. The authors thank the reviewer for the valuable comments on the manuscript.

References

[1] B.E. Conway, Electrochemical Supercapacitors: Scientific Fundamentals and Technological Applications, Kluwer Academic/Plenum Publishing, New York, 1999.
[2] R. Kötz, M. Carlen, Principles and applications of electrochemical capacitors, Electrochim. Acta 45 (2000) 2483–2498.
[3] C. Schmitt, H. Pröbstle, J. Fricke, Carbon cloth-reinforced and activated aerogel films for supercapacitors, J. Non-Cryst. Solids 285 (2001) 77–82.
[4] E. Frackowiak, F. Béguin, Electrochemical storage of energy in carbon nanotubes and nanostructured carbons, Carbon 40 (2002) 1775–1787.
[5] R.W. Pekala, J.C. Farmer, C.T. Alviso, T.D. Tran, S.T. Mayer, J.M. Miller, B. Dunn, Carbon aerogels for electrochemical applications, J. Non-Cryst. Solids 225 (1998) 74–80.
[6] O. Barbieri, M. Hahn, A. Herzog, R. Kötz, Capacitance limits of high surface area activated carbons for double layer capacitors, Carbon 43 (2005) 1303–1310.
[7] E. Frackowiak, F. Béguin, Carbon materials for the electrochemical storage of energy in capacitor, Carbon 39 (2001) 937–950.
[8] C. Lin, J.A. Ritter, B.N. Popov, Correlation of the double-layer capacitance with the pore structure of sol–gel derived carbon xerogels, J. Electrochem. Soc. 146 (1999) 3639–3643.
[9] G. Gryglewicz, J. Machnikowski, E. Lorenc-Grabowska, G. Lota, E. Frackowiak, Effect of pore size distribution of coal-based activated carbons on double layer capacitance, Electrochim. Acta 50 (2005) 1197–1206.

[10] K.L. Yang, T.Y. Ying, S. Yiacoumi, C. Tsouris, E.S. Vittoratos, Electrosorption of ions from aqueous solutions by carbon aerogel: an electrical double-layer model, Langmuir 17 (2001) 1961–1969.
[11] P. Simon, Y. Gogotsi, Materials for electrochemical capacitors, Nat. Mater. 7 (2008) 845–854 (and references therein).
[12] D. Qu, Studies of the activated carbons used in double-layer supercapacitors, J. Power Sources 109 (2002) 403–411.
[13] D. Lozano-Castelló, D. Cazorla-Amorós, A. Linares-Solano, S. Shiraishi, H. Kurihara, A. Oya, Influence of pore structure and surface chemistry on electric double layer capacitance in non-aqueous electrolyte, Carbon 41 (2003) 1765–1775.
[14] K. Okajima, K. Ohta, M. Sudoh, Capacitance behavior of activated carbon fibers with oxygen-plasma treatment, Electrochim. Acta 50 (2005) 2227–2231.
[15] C.T. Hsieh, H. Teng, Influence of oxygen treatment on electric double-layer capacitance of activated carbon fabrics, Carbon 40 (2002) 667–674.
[16] S. Yoon, J. Lee, T. Hyeon, S.M. Oh, Electric double-layer capacitor performance of a new mesoporous carbon, J. Electrochem. Soc. 147 (2002) 507–512.
[17] H.Y. Liu, K.P. Wangand, H. Teng, A simplified preparation of mesoporous carbon and the examination of the carbon accessibility for electric double layer formation, Carbon 43 (2005) 559–566.
[18] R.W. Pekala, Organic aerogels from the polycondensation of resorcinol with formaldehyde, J. Mater. Sci. 24 (9) (1989) 3221–3227.
[19] S.T. Mayer, J.L. Kaschmitter, R.W. Pekala, Method of low pressure and/or evaporative drying of aerogel, US Patent 5,420,168 (1995).
[20] T. Yamamoto, T. Sugimoto, T. Suzuki, S.R. Mukai, H. Tamon, Preparation and characterization of carbon cryogel microspheres, Carbon 40 (2002) 1345–1351.
[21] H. Darmstadt, C. Roy, S. Kaliaguine, S.H. Joo, R. Ryoo, Synthesis of new nanoporous carbon with hexagonally ordered mesostructure, J. Am. Chem. Soc. 122 (43) (2000) 1071–1072.
[22] M. Antonietti, Surfactants for novel templating applications, J. Colloid Interface Sci. 6 (2001) 244–248.
[23] C.T. Kresge, M.E. Leonowicz, W.J. Roth, J.C. Vartuli, J.S. Beck, Ordered mesoporous molecular sieves synthesized by a liquid-crystal template mechanism, Nature 359 (1992) 710–712.
[24] J.S. Beck, J.C. Vartuli, W.J. Roth, M.E. Leonowicz, C.T. Kresge, K.D. Schmitt, T.W. Chu, D.H. Olson, E.W. Sheppard, S.B. McCullen, J.B. Higgins, J.L. Schlenker, A new family of mesoporous molecular sieves prepared with liquid crystal templates, J. Am. Chem. Soc. 114 (1992) 10834–10843.
[25] J. Patarin, B. Lebeau, R. Zana, Recent advances in the formation mechanisms of organized mesoporous materials, J. Colloid Interface Sci. 7 (2002) 107–115.
[26] G.J.A.A. Soler-Illia, C. Sanchez, B. Lebeau, J. Patarin, Chemical strategies to design textured materials: from microporous and mesoporous oxides to nanonetworks and hierarchical structures, Chem. Rev. 102 (2002) 4093–4138.
[27] W. Bell, S. Dietz, Mesoporous carbon and polymers, US Patent 6,297,293 (2001).
[28] W.C. Oliver, G.M. Pharr, An improved technique for determining hardness and elastic modulus using load and displace sensing indentation experiments, J. Mater. Res. 7 (1992) 1564–1583.
[29] G.A. Planes, M.C. Miras, C.A. Barbero, Double layer properties of carbon aerogel electrodes measured by probe Beam deflection and ac impedance techniques, Chem. Commun. (2005) 2146–2148.
[30] M.T. Anderson, J.E. Martin, J.G. Odinek, P.P. Newcomer, Effect of methanol concentration on CTAB micellization and on the formation of surfactant-templated silica (STS), Chem. Mater. 10 (1998) 1490–1500.
[31] N. Nishiyama, T. Zheng, Y. Yamane, Y. Egashira, K. Ueyama, Microporous carbons prepared from cationic surfactant–resorcinol/formaldehyde composites, Carbon 43 (2005) 269–274.
[32] K.T. Lee, S.M. Oh, Novel synthesis of porous carbons with tunable pore size by surfactant-templated sol–gel process and carbonisation, Chem. Commun. (2002) 2722–2723.
[33] D. Fujikawa, M. Uota, T. Yoshimura, G. Sakai, T. Kijima, Shape-controlled synthesis of nanocarbons from resorcinol–formaldehyde nanopolymers using surfactant-templated vesicular assemblies, Carbon 45 (2007) 1289–1295.
[34] R. De Levie, On porous electrodes in electrolyte solutions, Electrochim. Acta 8 (1963) 751–780.
[35] R. De Levie, in: P. Delahay (Ed.), Advances in Electrochemistry and Electrochemical Engineering, vol. VI, John Wiley, New York, 1967, p. 329.
[36] M.M. Bruno, N.G. Cotella, M.C. Miras, C.A. Barbero, Porous carbon–carbon composite replicated from a natural fibre, Chem. Commun. (2005) 5896–5898.
[37] G.A. Planes, Thesis, Universidad Nacional de Río Cuarto, Argentina, 2003.
[38] T.Y. Ying, K.L. Yang, S. Yiacoumi, C. Tsouris, Electrosorption of ions from aqueous solutions by nanostructured carbon aerogel, J. Colloid Interface Sci. 250 (2002) 18–27.
[39] M. Hahn, M. Bärtschi, O. Barbieri, J.-C. Sauter, R. Kötz, R. Gallay, Interfacial capacitance and electronic conductance of activated carbon double-layer electrodes, Electrochem. Solid-State Lett. 7 (2) (2004) A33–A36.
[40] E. Lust, G. Nurk, A. Jänes, M. Arulepp, L. Permann, P. Nigu, P. Möller, Electrochemical properties of nanoporous carbon electrode, Condens. Matter. Phys. (2002) 307–327.
[41] A. Gupta, I.R. Harrison, Small-angle X-ray scattering (SAXS) in carbonized phenolic resins, Carbon 32 (1994) 953–960.
[42] M.C. Roman-Martínez, D. Cazorla-Amoros, A. Linares-Solano, C. Salinas-Martinez de Lecea, F. Atamny, Structural study of a phenol formaldehyde char, Carbon 34 (1996) 719–727.
[43] P. Diss, J. Lamon, L. Carpentier, J.L. Loubet, P.h. Kapsa, Sharp indentation behavior of carbon/carbon composites and varieties of carbon, Carbon 40 (2002) 2567–2579.
[44] N.A. Fleck, H. Otoyo, A. Needleman, Indentation on porous solids, Int. J. Solids Struct. 26 (13) (1992) 1613–1636.
[45] A.A. Volinsky, J.B. Vella, W.W. Gerberich, Fracture toughness, adhesion and mechanical properties of low-K dielectric thin films measured by nanoindentation, Thin Solid Films 429 (2003) 201–210.
[46] X. Chen, Y. Xiang, J.J. Vlassak, Novel technique for measuring the mechanical properties of porous materials by nanoindentation, J. Mater. Res. 21 (3) (2006) 715–724.
[47] X. Chen, R. Wang, N. Yao, A.G. Evans, J.W. Hutchinson, R.W. Bruce, Foreign object damage in a thermal barrier system: mechanisms and simulations, Mater. Sci. Eng. A352 (2003) 221–231.
[48] J.S. Fields, M.V. Swain, The indentation characterization of the mechanical properties of various carbon materials: glassy carbon, coke and pyrolytic graphite, Carbon 34 (1996) 1357–1366.
[49] S. Yoon, J. Lee, T. Hyeon, S. Oh, Electric double-layer capacitor performance of a new mesoporous carbon, J. Electrochem. Soc. 147 (2000) 2507–2512.
[50] M. Kanari, K. Tanaka, S. Baba, M. Eto, Nanoindentation behavior of a two-dimensional carbon–carbon composite for nuclear applications, Carbon 35 (1997) 1429–1437.
[51] W.C. Oliver, G.M. Pharr, Measurement of hardness and elastic modulus by instrumented indentation: advances in understanding and refinements to methodology, J. Mater. Res. 19 (2004) 3–21.
[52] D.T. Marx, L. Rieste, Mechanical properties of carbon–carbon composite components determined using nanoindentation, Carbon 37 (1999) 1679–1684.
[53] C.C. Charms, J.W. Weber, D.M. Petels, K.L. Thomas (Eds.), Engineers guide to composite materials, Am. Soc. Met. (1987) 3–11.
[54] M.G. Rodrigues, N.C. Da Cruz, E.C. Rangel, R.L. Zimmerman, D. Ila, D.B. Poker, D.K. Hensley, Nanoindentation mechanical properties characterization of glassy polymeric carbon treated with ion beam, Nucl. Instrum. Methods B 191 (2002) 524–529.
[55] T. Woignier, J. Reynes, A. Hafidi Alaoui, I. Beurroies, J. Phalippou, Different kinds of structure in aerogels: relationships with the mechanical properties, J. Non-Cryst. Solids 241 (1998) 45–52.
[56] A.R. Boccaccin, New approach for the Young's modulus-porosity correlation of ceramic materials, Ceram. Int. 23 (1997) 239–245.
[57] L. Gibson, M. Ashby, Cellular Solids, 2nd, Cambridge University Press, New York, 1997.
[58] R.W. Rice, Evaluation and extension of physical property-porosity models based on minimum solid area, J. Mater. Sci. 31 (1996) 102–118.
[59] R.W. Rice, Comparison of physical property-porosity behaviour with minimum solid area models, J. Mater. Sci. 31 (1996) 1509–1528.